Electronic Supplementary Material (ESI) for RSC Advances.
This journal is © The Royal Society of Chemistry 2016

Supporting Information

Insights into the electrooptical anion sensing properties of a new organic receptor: Solvent dependent chromogenic response and DFT studies

Srikala P.,[a] Kartick Tarafdar[b] , A. Nityananda Shetty[c] and Darshak R. Trivedi[a*]

[a]*Supramolecular Chemistry Laboratory, National Institute of Technology Karnataka (NITK), Surathkal-575025, Karnataka, India*

[b]*Department of Physics, National Institute of Technology Karnataka (NITK), Surathkal-575025, Karnataka, India*

[c]*Department of Chemistry, National Institute of Technology Karnataka (NITK), Surathkal-575025, Karnataka, India*

[*]*Author to whom correspondence should be addressed* e-mail: darshak_rtrivedi@yahoo.co.in,

, Tel.: +91-824-2473205; fax: +91 824 2474033.

Table of contents

1 Experimental section
2 **Fig. S1**: FTIR spectrum of Receptor R
3 **Fig. S2:** ^{1}H-NMR spectrum of receptor R
4 **Fig. S3**: Mass spectrum of receptor R
5 **Fig. S4 :** UV-Vis absorption spectra of R(1×10^{-4} in dry DMSO) upon addition of 1 eq. of TBA salts of anions
6 **Fig. S5**: Colour change of the receptor with the addition of 1eq.of TBA salts of anions
7 **Fig. S6:** UV-Vis absorption spectra of R(DMSO/Tris HCl (9:1 v/v, 10 ^{4}M) upon addition of 2 eq. of TBA salts of anions
8 **Fig. S7:** UV-Vis titration spectra of R (1×10^{-4} M in dry DMSO) with the incremental addition of standard solution of TBAAcO (1×10^{2}M in dry DMSO
9 **Fig. S8:** B-H plot of receptor R- TBAAcO complex in dry DMSO
10 **Fig. S9:** UV-Vis titration spectra of R (1×10^{-4} M in dry DMSO) with the incremental addition of standard solution of $TBAH_2PO_4$ (1×10^{2}M in dry DMSO)
11 **Fig. S10:** B-H plot of receptor R- TBA H_2PO_4 complex in dry DMSO
12 **Fig. S11:** UV-Vis titration spectra of R (1×10^{-4} M in dry DMSO) with the incremental addition of standard solution of TBAF (1×10^{2}M in dry DMSO)
13 **Fig. S12:** B-H plot of receptor R- TBAF complex in dry DMSO
14 **Fig. S13:** B-H plot of receptor R- TBAAcO complex in Tris HCl buffer
15 **Fig. S14:** UV-Vis absorption spectra of receptor (1×10^{-4}M) in various polar aprotic solvents with the addition of 1 eq. of TBAAcO
16 **Fig. S15:** UV-Vis spectra of R (1×10^{-4} M in THF) upon addition of 1 eq. of TBA salts of F , AcO and H_2PO_4 ions
17 **Fig. S16:** Colour change of R (1×10^{-4} M in THF) upon addition of 1 eq. of F , AcO and H_2PO_4
18 **Fig. S17:**Solvatochromic effect observed with the addition of 1 eq. of $TBAH_2PO_4$ to receptor solution (1×10 -4 M) in various polar aprotic solvents
19 **Fig. S18:** Solvatochromic effect observed with the addition of 1 eq. of TBAF to receptor solution (1×10^{-4} M) in various polar aprotic solvents
20 **Fig. S19:** UV-Vis titration spectra of R(1×10^{-4} M, 9:1 v/v DMSO/H_2O) with the incremental addition of standard solution of NaF
21 **Fig. S20:** B-H plot of receptor R- Na^{+} F complex in aqueous media
22 **Fig. S21:**UV-Vis titration spectra of R(1×10^{-4} M, 9:1 v/v DMSO/H_2O) with the incremental addition of standard solution of NaAcO
23 **Fig. S22:**B-H plot of receptor R- Na^{+} AcO complex
24 **Fig. S23:** UV-Vis spectra of R (1×10^{-4} M in DMSO) upon addition of a drop of mouthwash, seawater and vinegar
25 **Fig. S24:** Color change of R (1×10^{-4} M in DMSO) upon addition of a drop of mouthwash, seawater and vinegar
26 **Fig. S25:** Color change of Receptor R upon dry grinding of receptor with 1 eq. of TBAAcO
27 **Fig. S26:** Cyclic voltammogram of Receptor R ($5x10^{-5}$M) with incremental addition of TBAAcO ion
28 **Fig. S27:** ^{1}H NMR titration of receptor R with incremental addition of TBAOH ion
29 **Fig. S28:** UV-Vis titration spectra of R(1×10^{-4} M, DMSO) with the incremental addition of standard solution of TBAOH (1×10^{2}M in DMSO)
30 **Fig. S29:** Optimized geometry of the receptor in gas phase
31 **Fig. S30:** HOMO of the receptor in gas phase
32 **Fig. S31:** LUMO of the receptor in gas phase
33 **Fig. S32:** Optimized structure of the receptor in DMSO

Fig. S33: HOMO of the receptor in DMSO
Fig. S34: LUMO of the receptor in DMSO
Fig. S35: Optimized structure of deprotonated receptor in acetone
Fig. S36: HOMO of the deprotonated receptor in acetone
Fig. S37: LUMO of the deprotonated receptor in acetone
Fig. S38: DFT derived UV-Vis spectra of the receptor in gas phase, in solvents such as DCM and acetone with addition of AcO^- ion
Table S1: Changes in absorption maxima of receptor R in various solvents upon addition of 1eq. of TBAAcO in dry DMSO
Table S2: Binding ratio, binding constant and detection limit of receptor R
Table S3: Mullliken charge distribution and spin densities derived from DFT calculations

Experimental section:

Materials and methods:

All the chemicals used in the present study were procured from Sigma-Aldrich and Alfa Aesar and were used as received without further purification. All the solvents were purchased from SD Fine, India, were of HPLC grade and used without further distillation.
Melting point was measured on Stuart SMP3 melting-point apparatus in open capillaries. Infrared spectrum was recorded on Bruker Apex FTIR spectrometer. UV-Vis spectroscopy was performed with analytik jena Specord S600 spectrometer in standard 3.0 mL quartz cell with 1cm path length. The ^{1}H NMR spectra were recorded on Bruker Ascend (400 MHz) instrument using TMS as internal reference and DMSO-d_6 as solvent. Resonance multiplicities are described as s (singlet), d (doublet), t (triplet) and m (multiplet). Mass spectrum was recorded on Bruker Daltonics *ESI* Q TOF. Cyclic voltammogram was recorded on Ivium electrochemical workstation (Vertex) at a scan rate of 20 mV/s with the potential range 1.0 mV to -1.0 mV.

We have performed the Density Functional Theory (DFT) simulation on the receptor molecule using GAUSSIAN 09 package. A closed shell Becke–Lee–Yang–Parr hybrid exchange-correlation three-parameter functional (B3LYP)[1-3] along with 6-311++G(d) basis set were used in the simulation to derive a complete geometry optimization for isolated receptor and its deprotonated form in the binding process. Berny's optimization algorithm was used to fully optimize the molecular geometry, which involves redundant internal coordinates. To confirm the convergence to the minima on the potential energy surface, the harmonic vibrational wavenumbers were calculated using analytic second derivatives and properly scale down to control the systematic errors caused by incompleteness of the basis set. In a second step the time dependent DFT (TD-DFT) method were used considering the same B3LYP exchange-correlation functional with 6-311++G (d,p) basis set to obtain the UV-Visible absorption spectra of free and deprotonated receptor.

Synthesis of (E)-1-(4-nitrobenzylidene)-2-(2,4-dinitrophenyl)hydrazine:
4-nitrobenzaldehyde (0.05 g, 0.33 mmol) and 2,4-dinitrophenylhydrazine(0.65 g, 0.33 mmol) were mixed in 5 ml ethanol. A drop of acetic acid was added and the reaction mixture was refluxed at 60^{o}C for 5 h. The formation of the product was confirmed through TLC by the generation of single spot indicative of the disappearance of starting materials.

Yield: 85%., m. p. 280 ^{o}C.

^{1}H NMR (DMSO- d_6, 400 MHz, ppm): δ 8.05 (s, H), 8.16 (s, H), 8.32-8.41 (m, 4H), 8.8 (s 1H), 8.86 (s, 1H), 11.85 (s 1H).

FTIR (KBr)(cm^{-1}): 3279(NH), 3089(Ar-CH), 1613(CH=N), 1510(C=C), 1331(NO_2), 1088(C-H)

Mass (ESI): m/z Calculated: 331.06 Obtained: 338($M+N^+$)

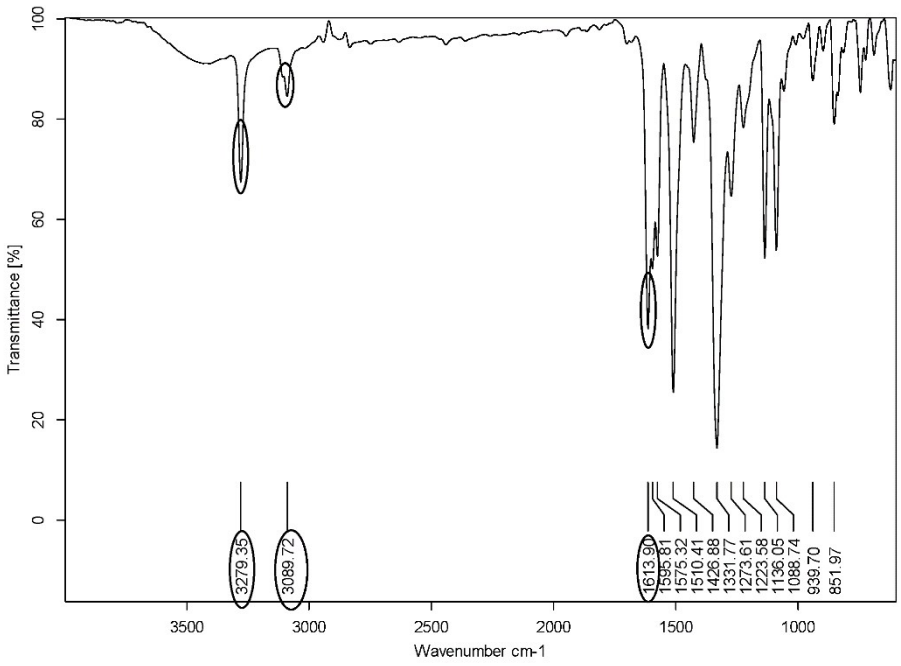

Fig. S1: FTIR spectrum of receptor R

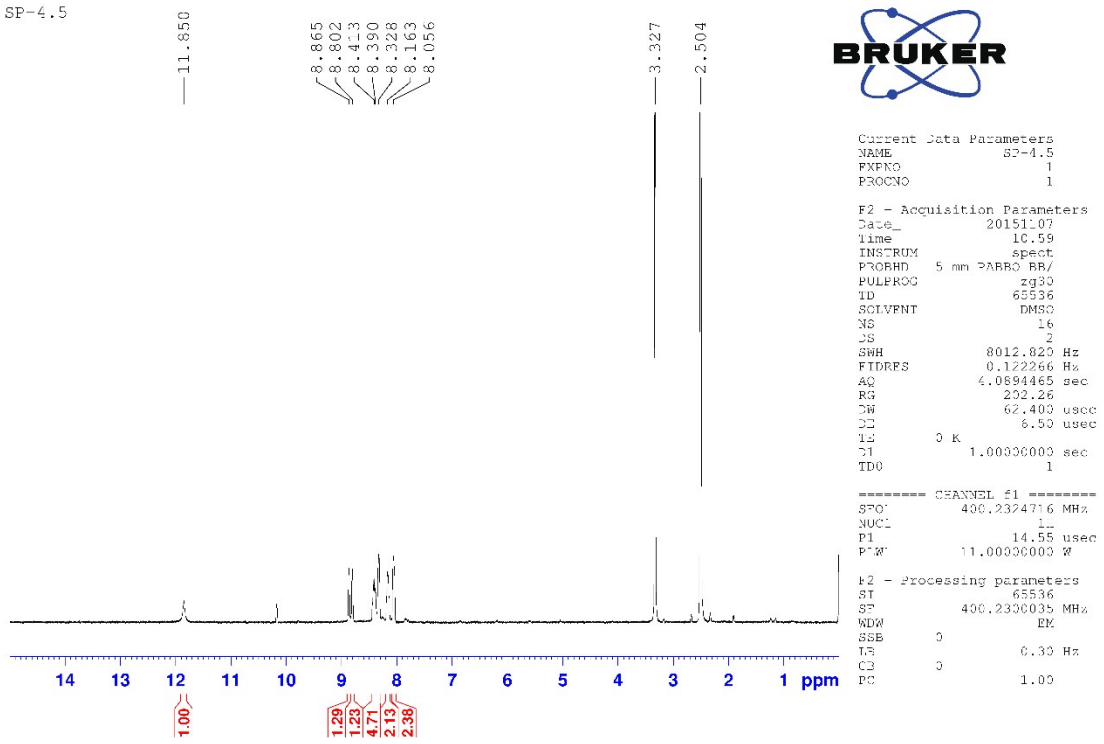

Fig S2: ^{1}H-NMR spectrum of receptor R

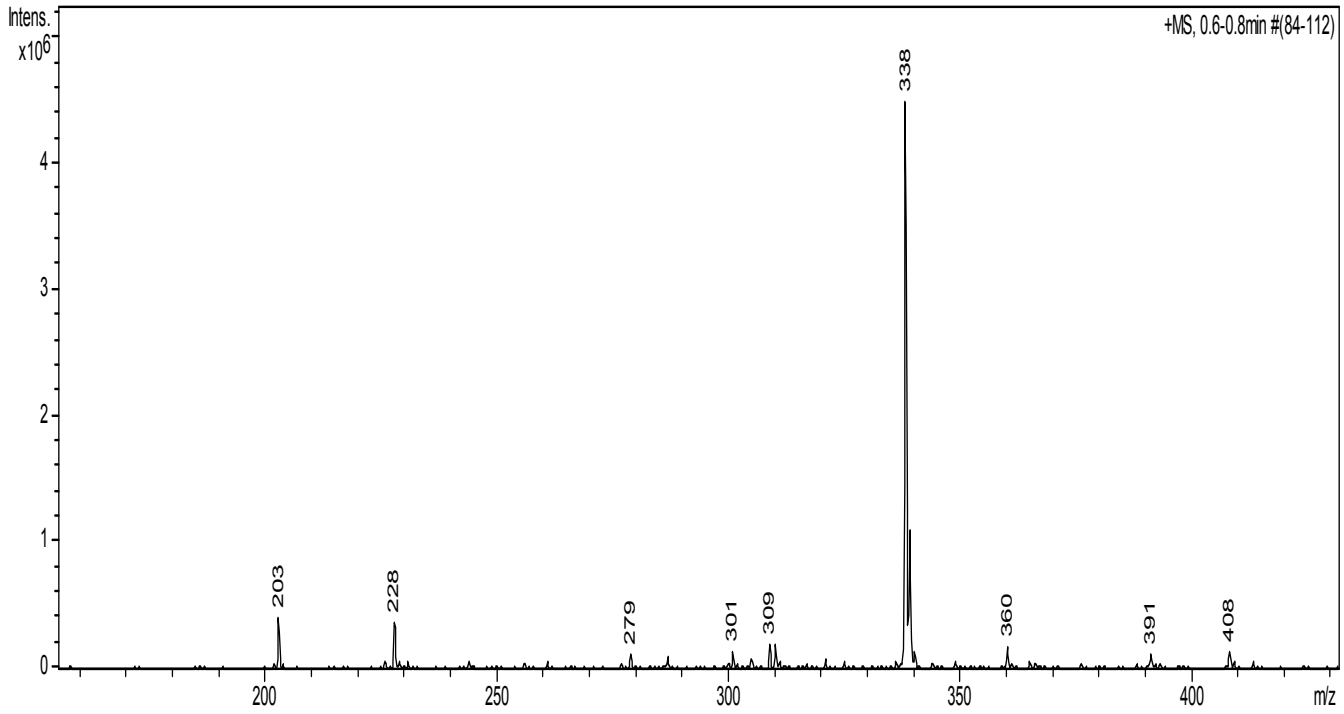

Fig S3: Mass spectrum of receptor R

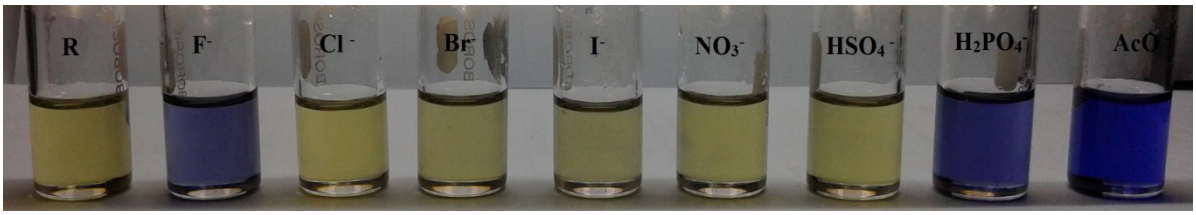

Fig. S4: Colour change of the receptor with the addition of 1eq.of TBA salts of anions

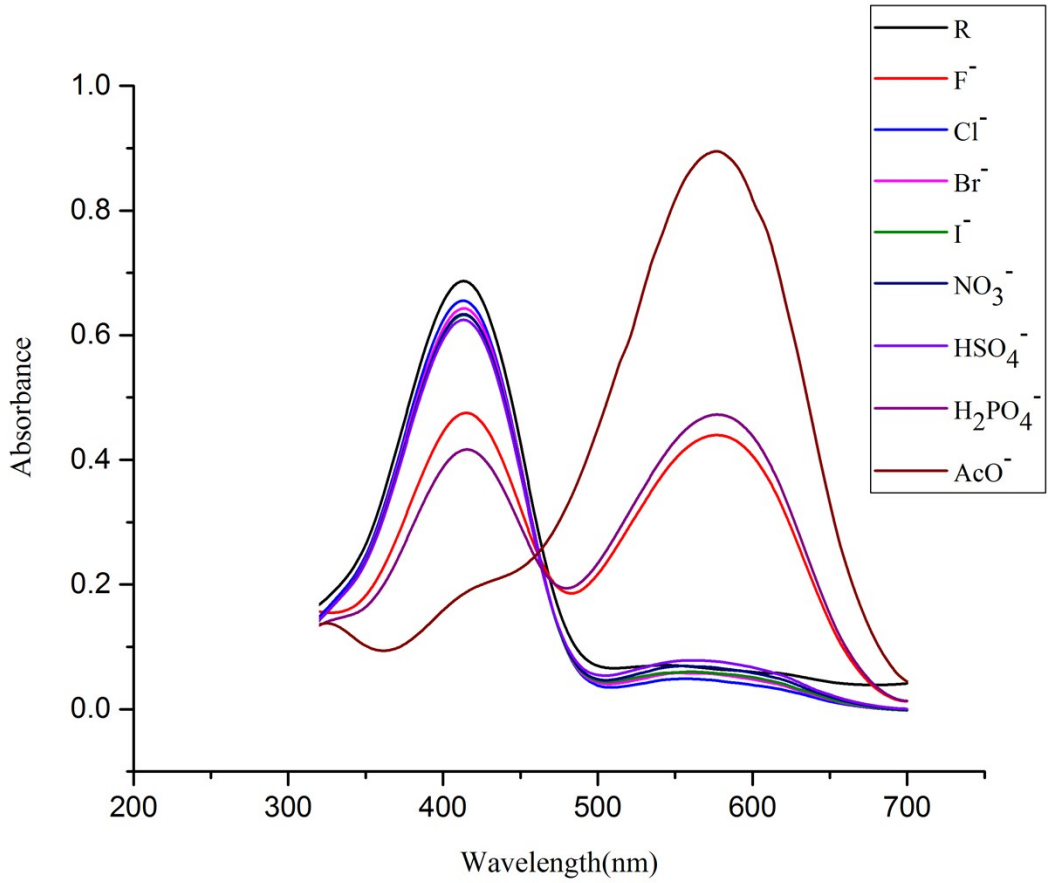

Fig. S5: UV-Vis absorption spectra of R(1×10^{-4} in dry DMSO) upon addition of 1 eq. of TBA salts of anions

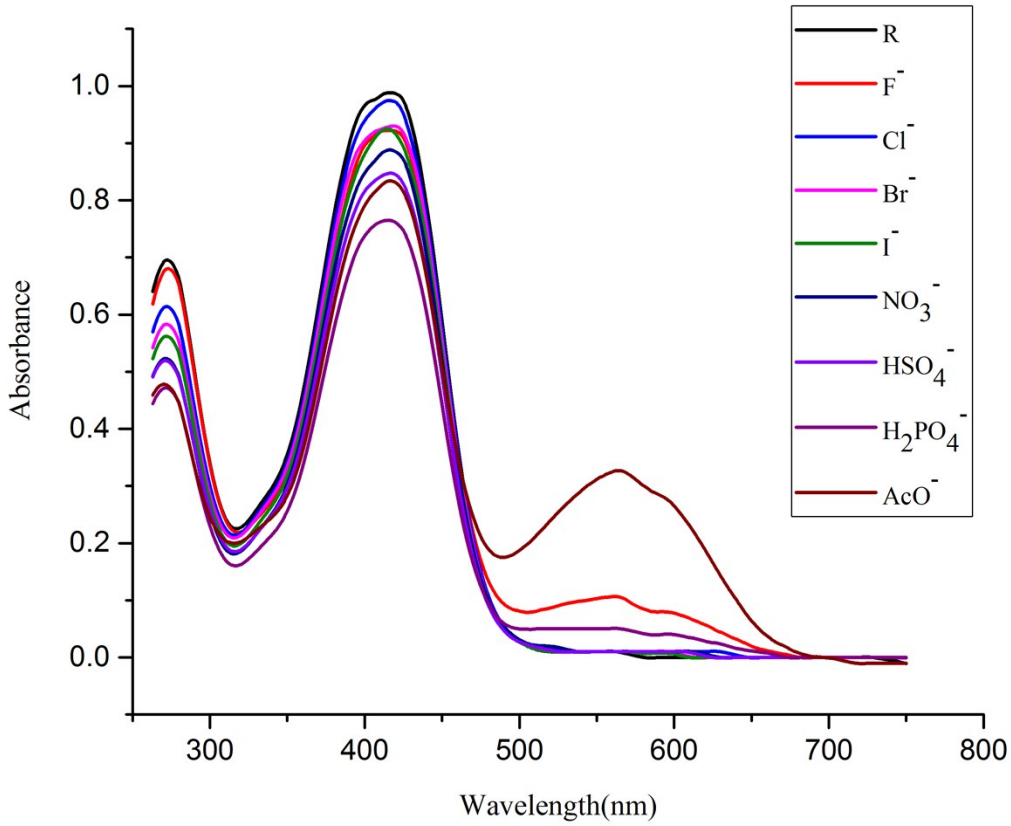

Fig. S6: UV-Vis absorption spectra of R (DMSO/Tris HCl (9:1 v/v, 10 ^{4}M) upon addition of 2 eq. of TBA salts of anions

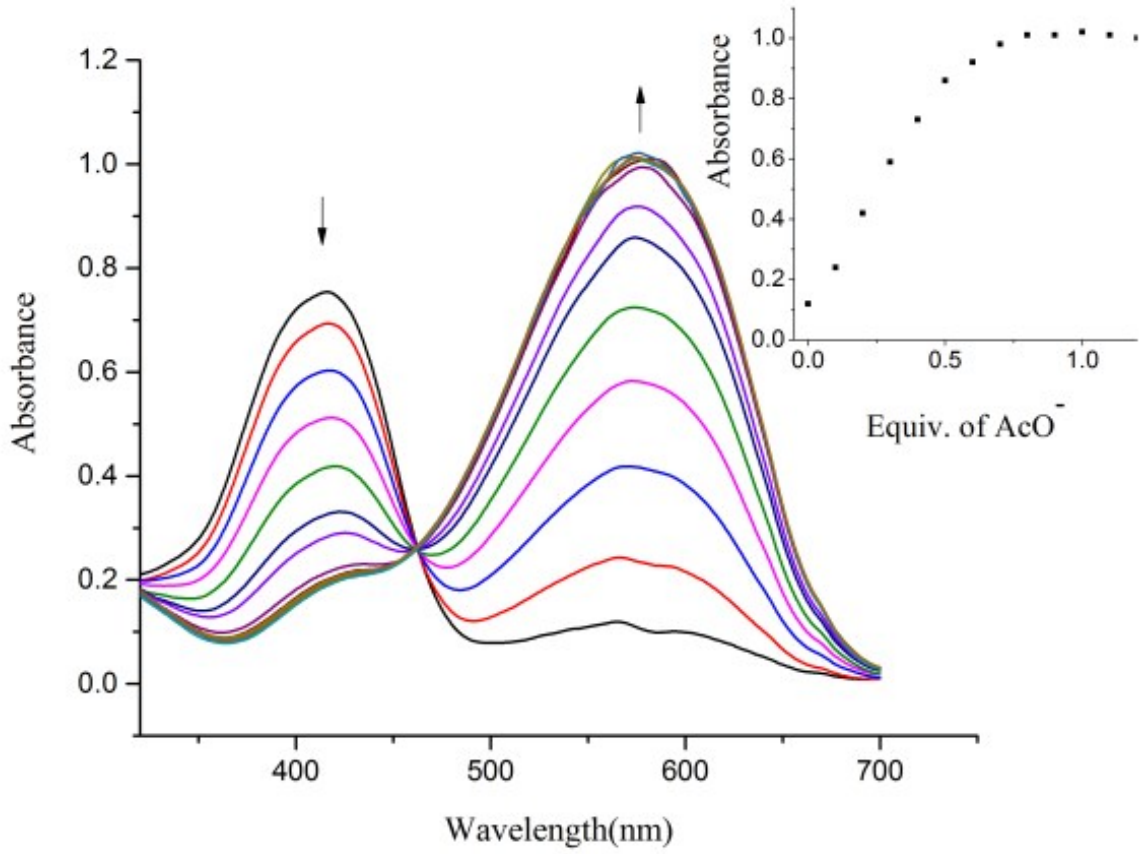

Fig. S7: UV-Vis titration spectra of R (1×10^{-4} M in dry DMSO) with the incremental addition of standard solution of TBAAcO (1×10^{-2}M in dry DMSO). Inset showing the binding isotherm at 572 nm

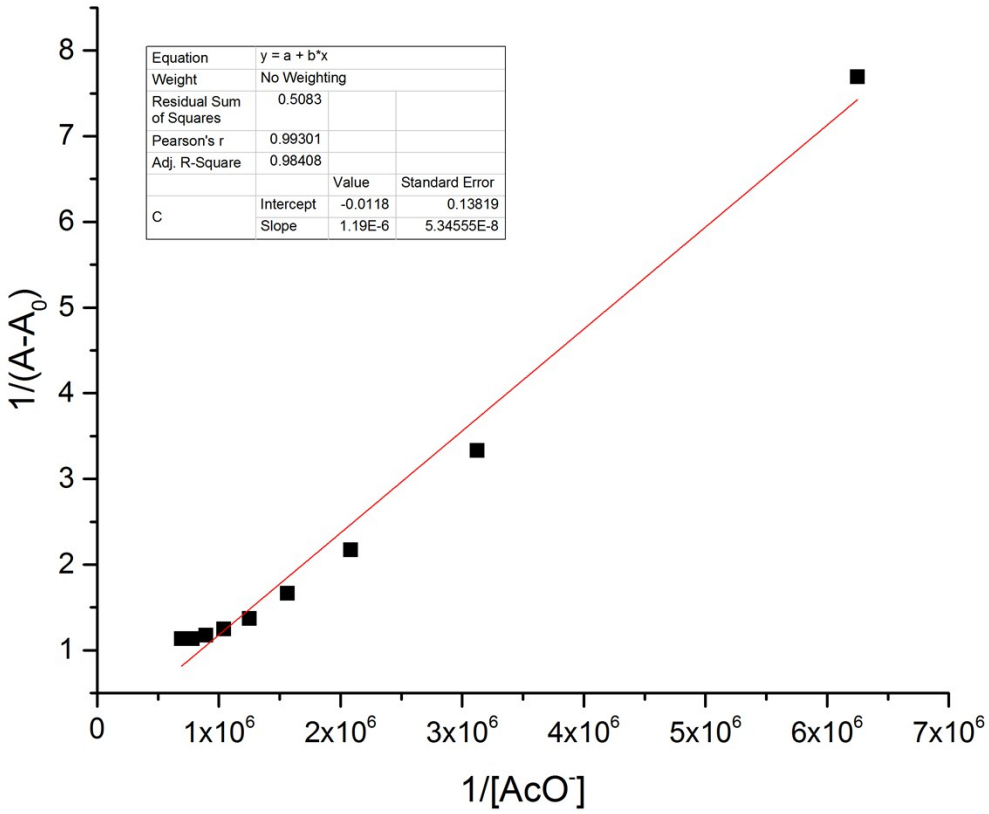

Fig. S8: B-H plot of receptor R- TBAAcO complex at a selected wavelength of 572 nm

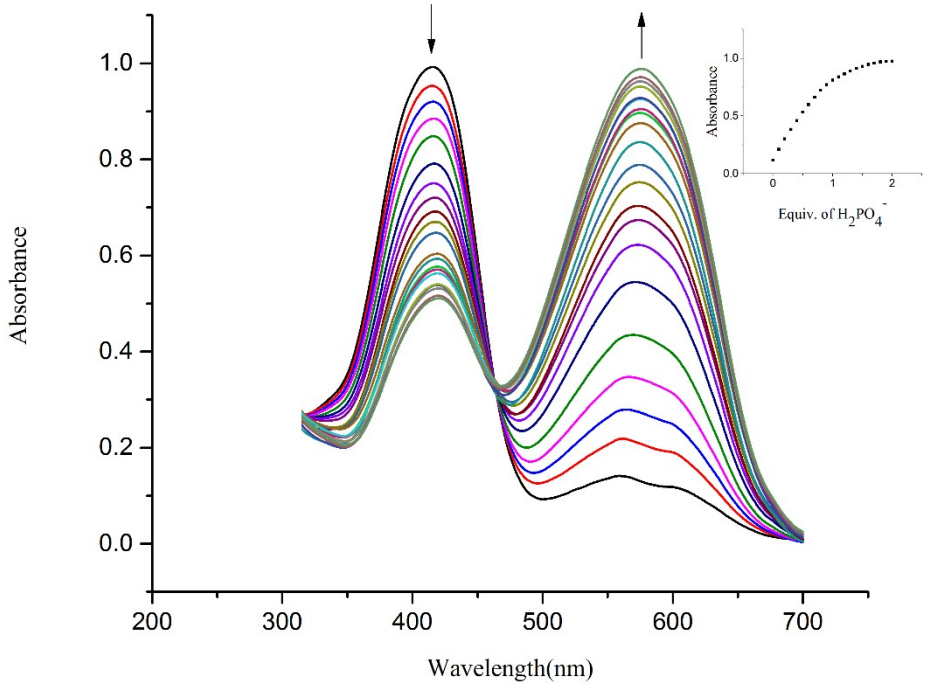

Fig. S9: UV-Vis titration spectra of R (1×10^{-4} M in dry DMSO) with the incremental addition of standard solution of $TBAH_2PO_4$ (1×10^{-2}M in dry DMSO). Inset showing the binding isotherm at 572 nm

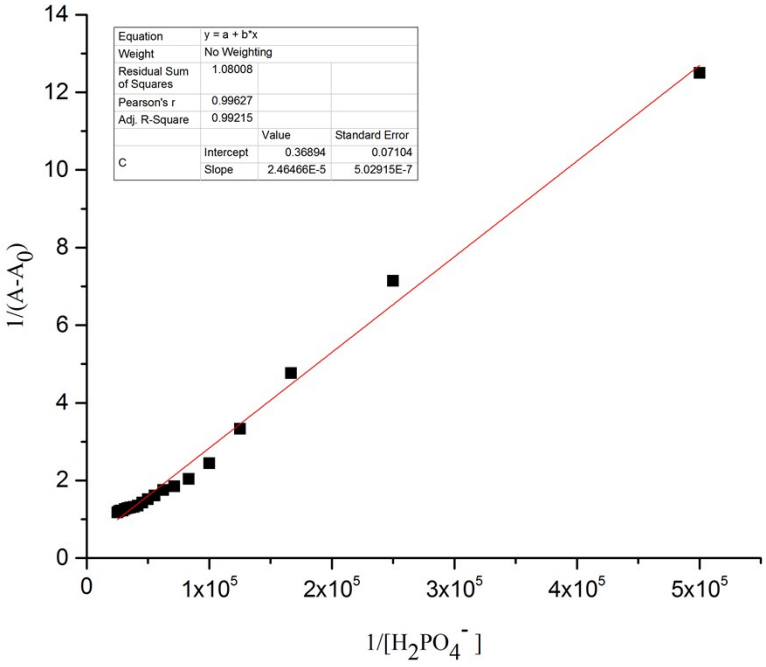

Fig. S10: B-H plot of receptor R- $TBAH_2PO_4$ complex at a selected wavelength of 572 nm

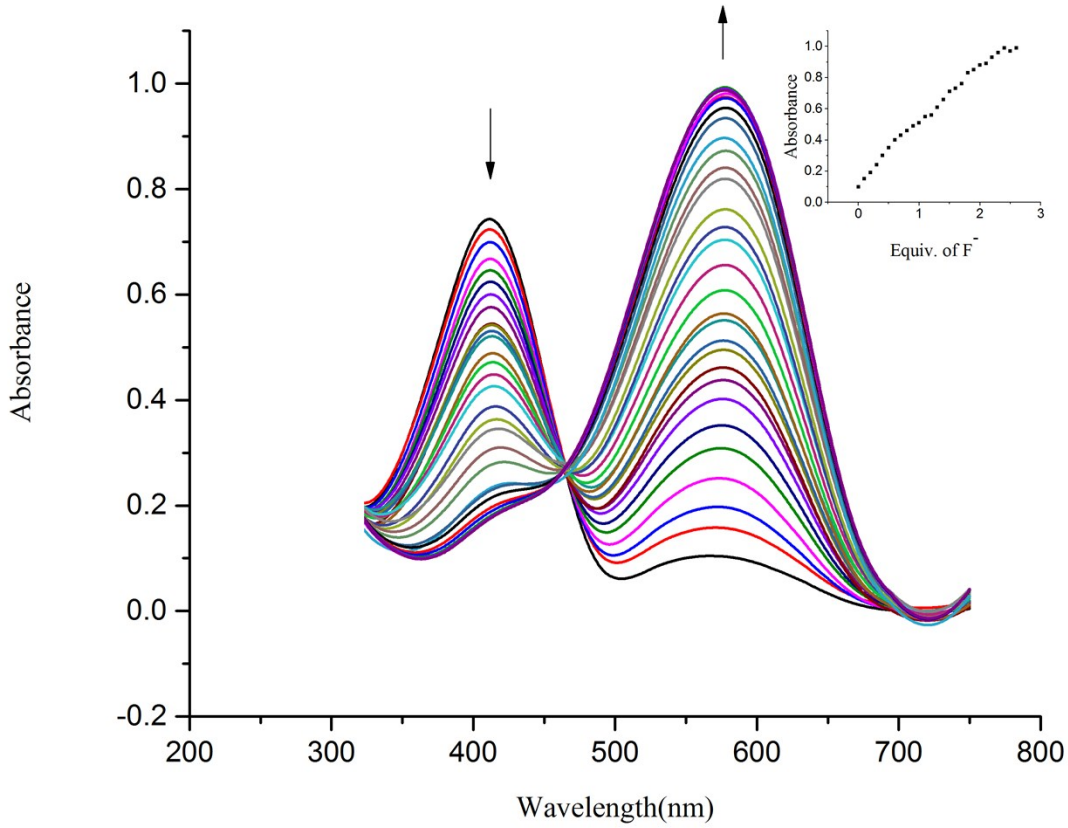

Fig. S11: UV-Vis titration spectra of R (1×10^{-4} M in dry DMSO) with the incremental addition of standard solution of TBAF (1×10^{-2}M in dry DMSO). Inset showing the binding isotherm at 578 nm

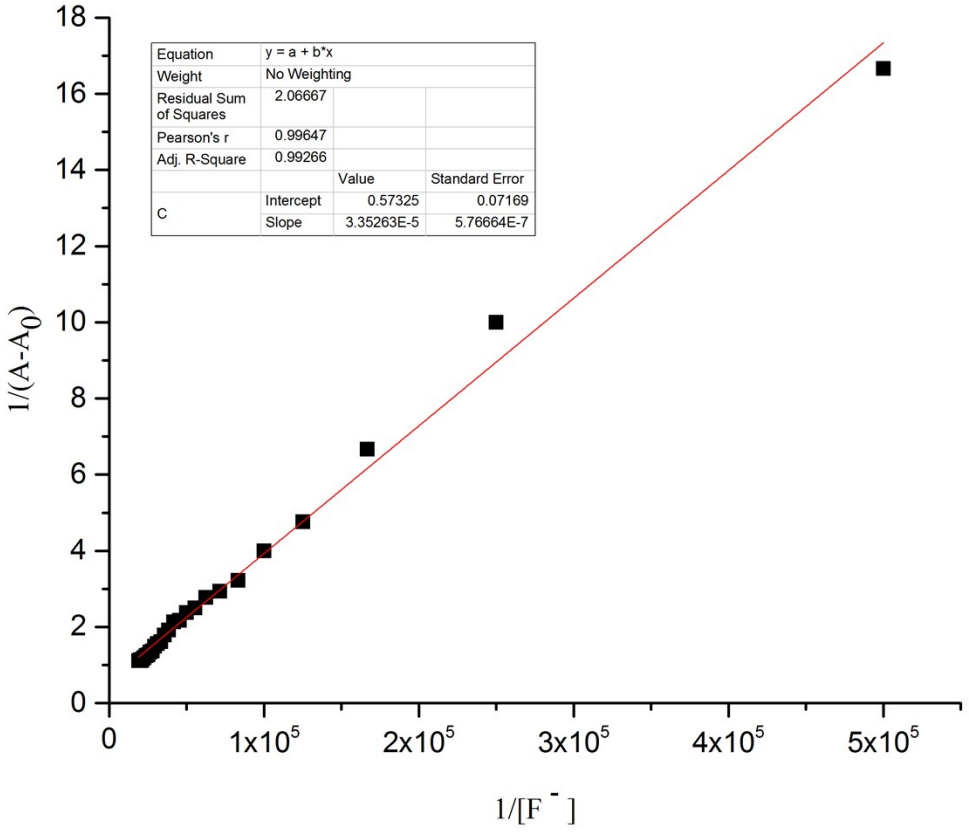

Fig. S12: B-H plot of receptor R- TBAF complex at a selected wavelength of 578 nm

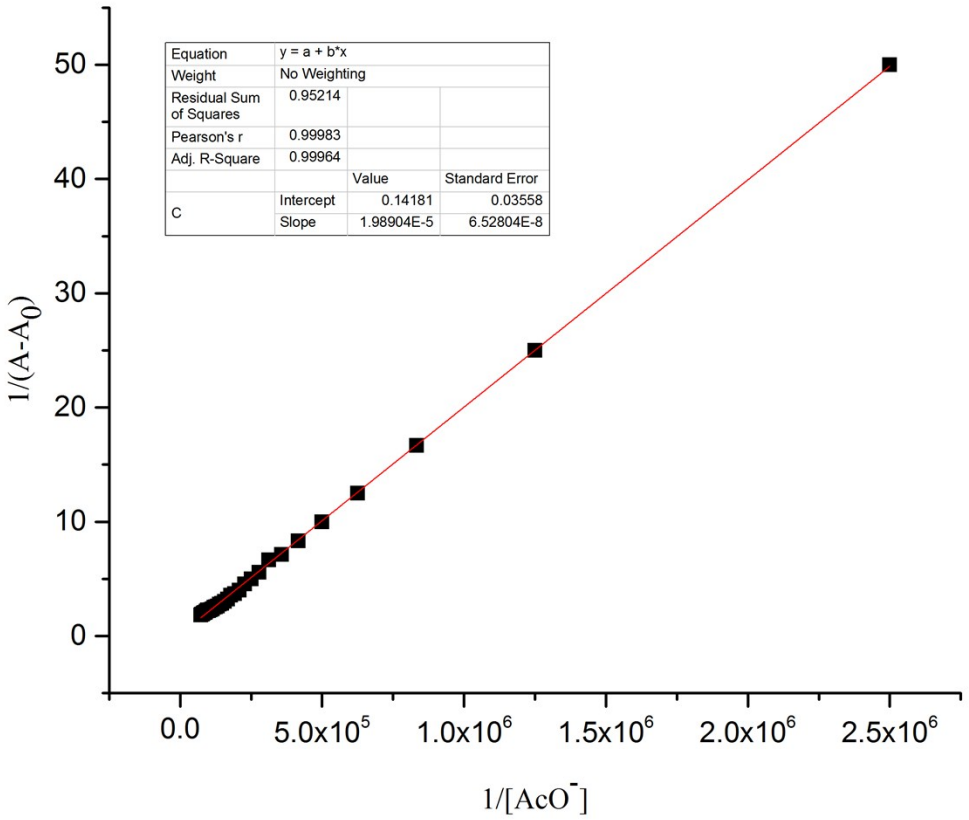

Fig. S13: B-H plot of receptor R- TBAAcO complex (buffer media) at a selected wavelength of 569 nm

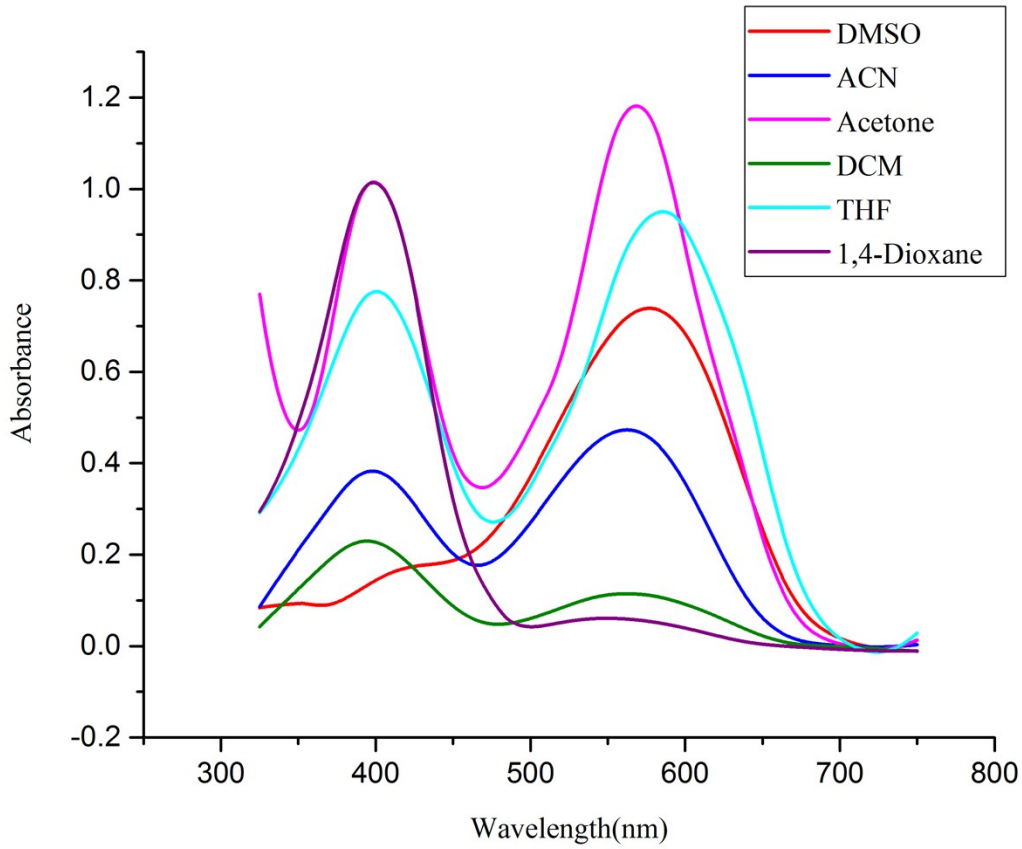

Fig. S14: UV-Vis absorption spectra of receptor (1×10^{-4}M) in various polar aprotic solvents with the addition of 1 eq. of TBAAcO (10^{-2} M in dry DMSO)

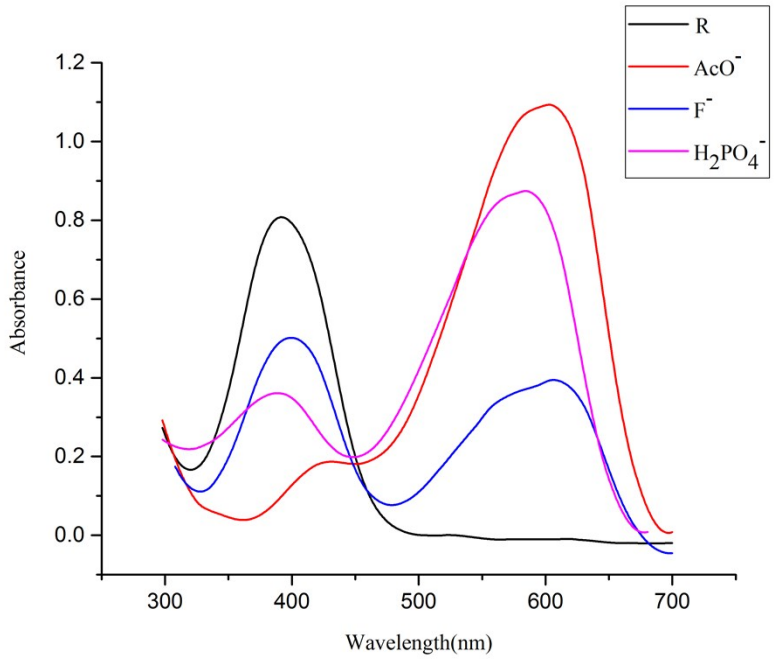

Fig.S15: UV-Vis spectra of R (1×10^{-4} M in THF) upon addition of 1 eq. of TBA salts of F^-, AcO^- and $H_2PO_4^-$ ions(1×10^{-2} M in dry DMSO)

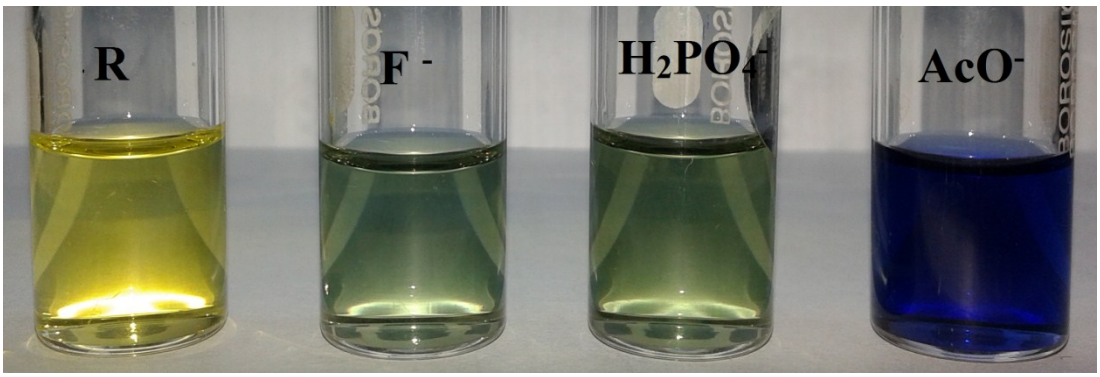

Fig.S16: Colour change of R (1×10^{-4} M in THF) upon addition of 1 eq. of F^-, AcO^- and $H_2PO_4^-$ (1×10^{-2} M as TBA salts in dry DMSO)

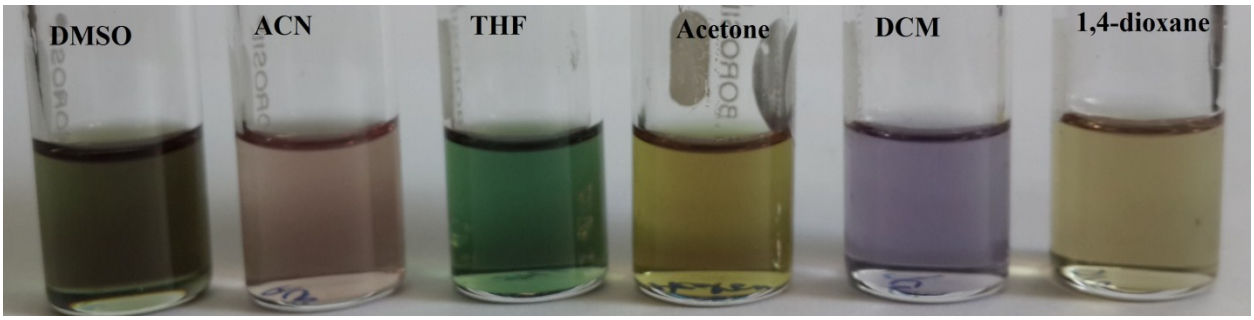

Fig. S17: Solvatochromic effect observed with the addition of 1 eq. of $TBAH_2PO_4$ to receptor solution (1×10^{-4} M) in various polar aprotic solvents

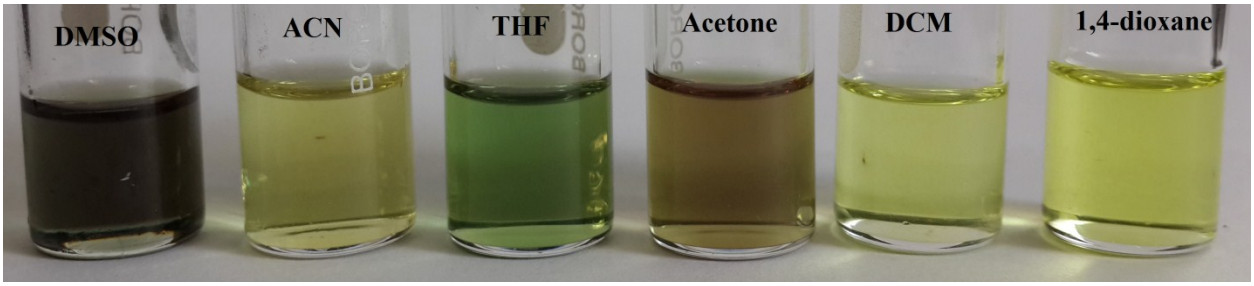

Fig. S18: Solvatochromic effect observed with the addition of 1 eq. of TBAF to receptor solution (1×10^{-4} M) in various polar aprotic solvents

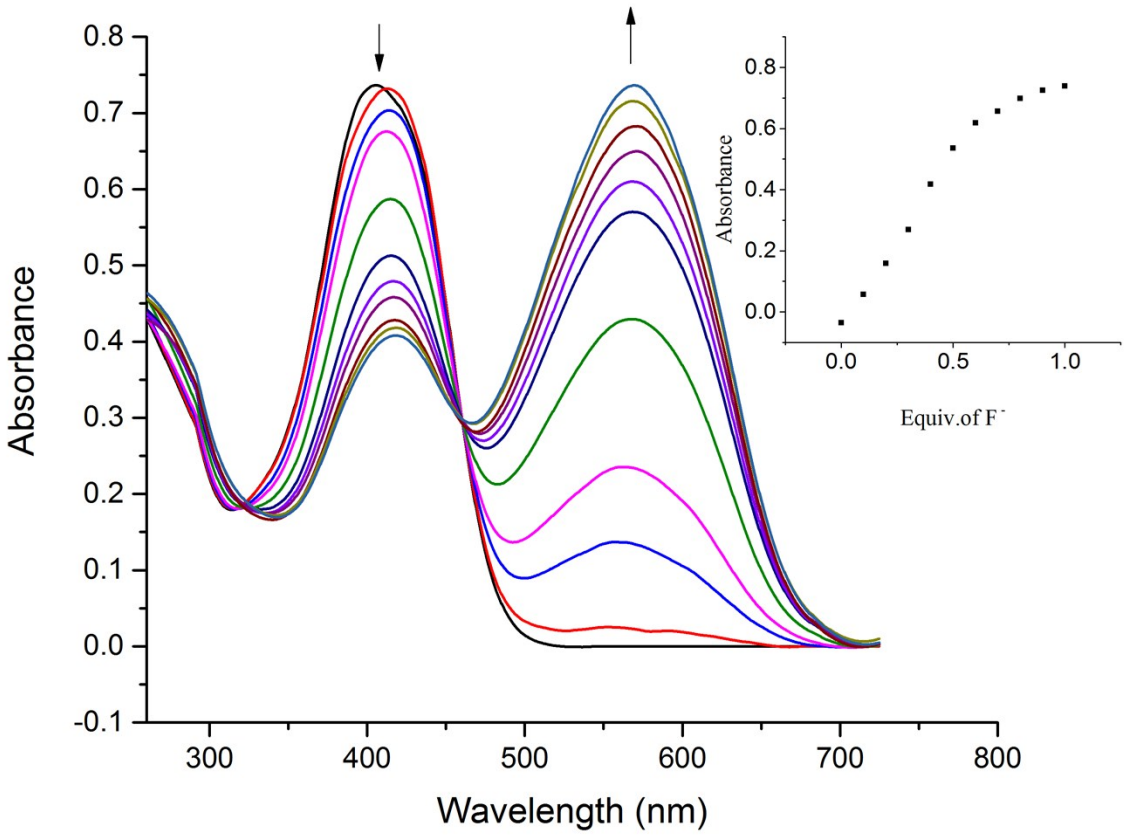

Fig.S19: UV-Vis titration spectra of R(1×10^{-4} M, 9:1, v/v DMSO/H_2O) with the incremental addition of standard solution of NaF (1×10^{-2}M in distilled water). Inset showing binding isotherm at 575 nm

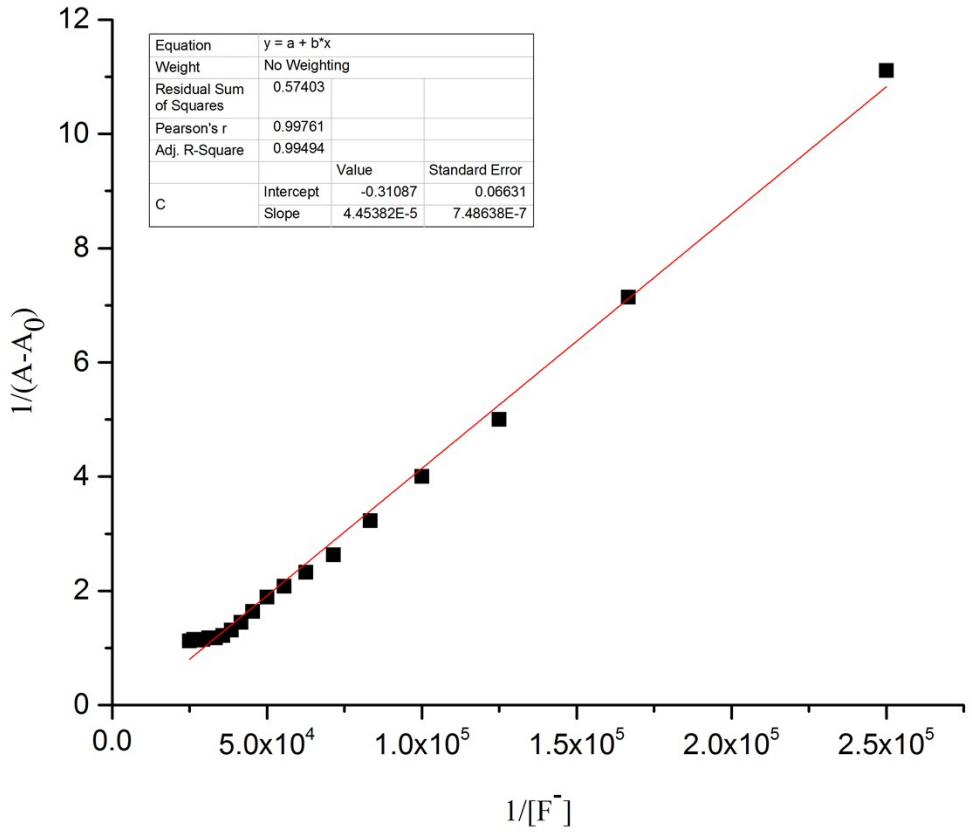

Fig.S20: B-H plot of receptor R- Na^+ F complex at a selected wavelength of 575 nm

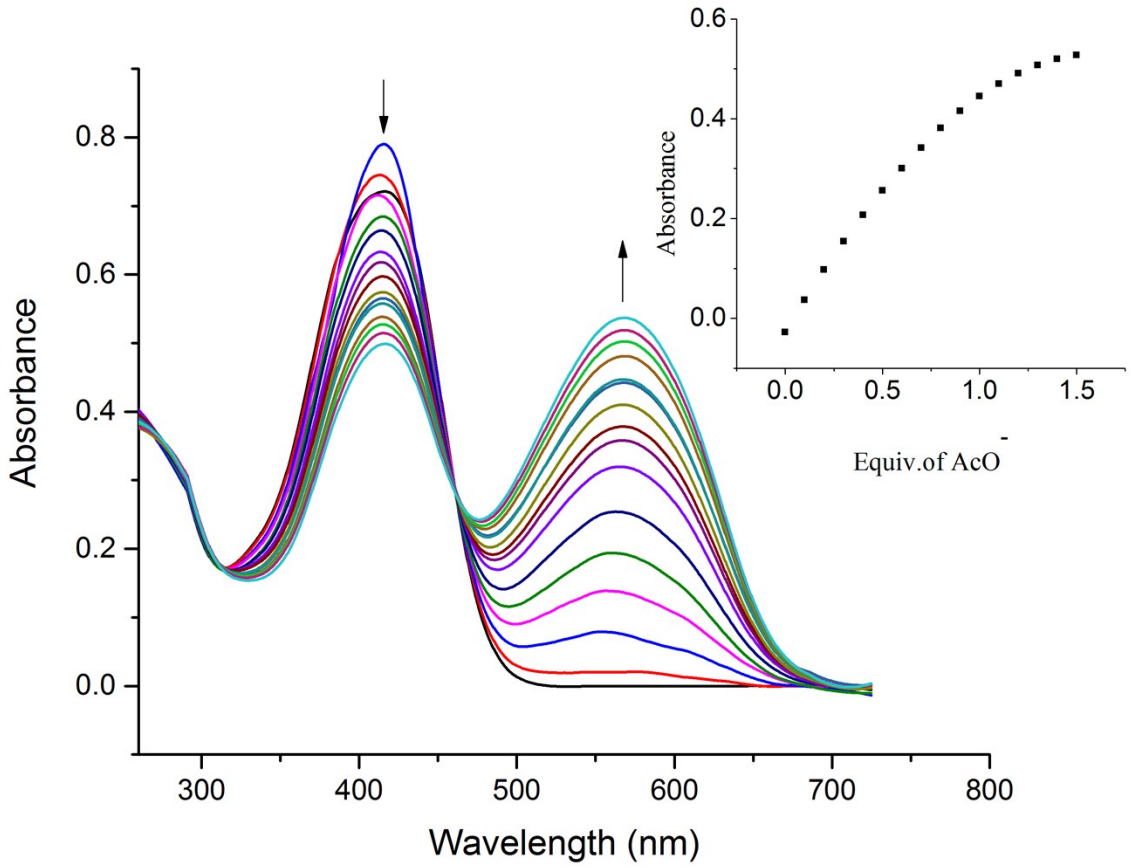

Fig.S21: UV-Vis titration spectra of R(1×10^{-4} M, 9:1, v/v DMSO/H_2O) with the incremental addition of standard solution of NaAcO (1×10^{-2}M in distilled water). Inset showing binding isotherm at 574nm

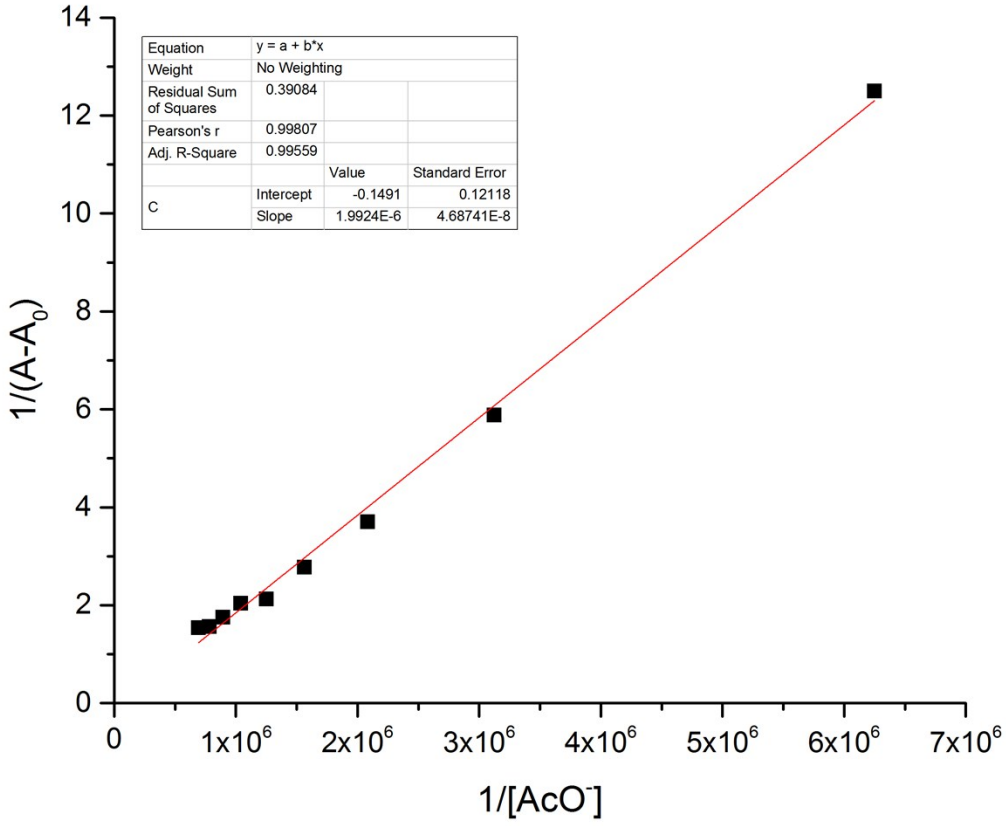

Fig.S22: B-H plot of receptor R- Na^+ AcO complex at a selected wavelength of 574 nm

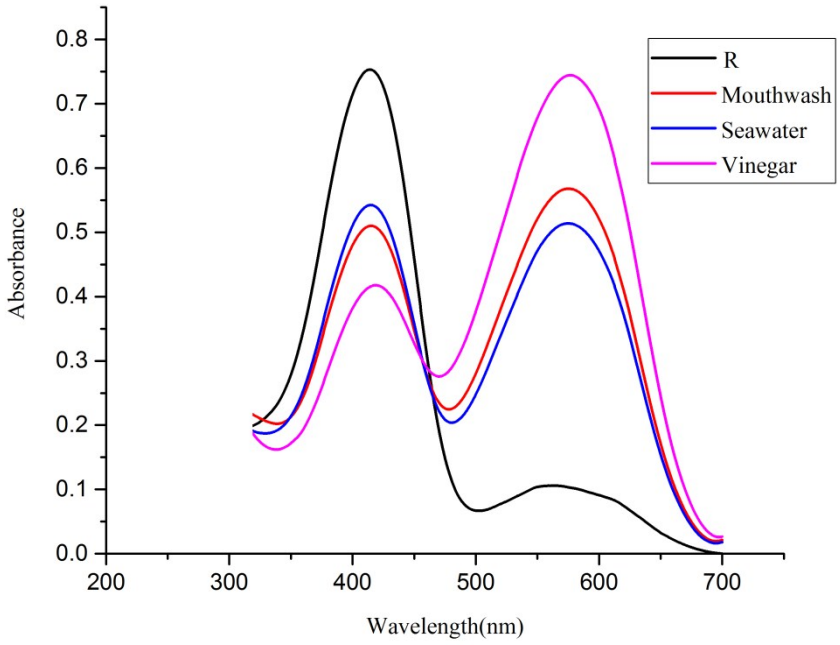

Fig.S23: UV-Vis spectra of R (1×10^{-4} M in DMSO) upon addition of a drop of mouthwash, seawater and vinegar

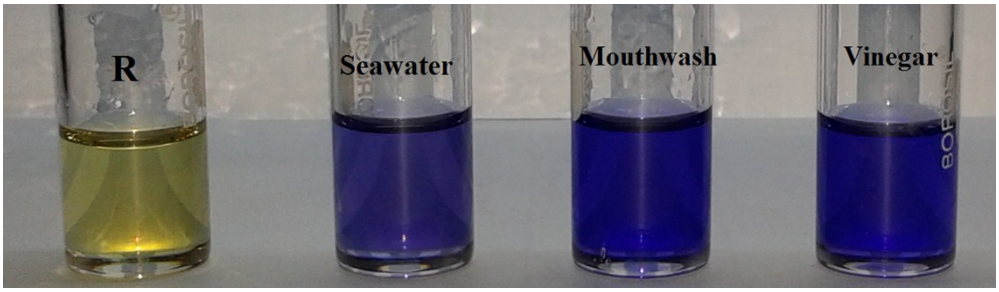

Fig.S24: Color change of R (1×10^{-4} M in DMSO) upon addition of a drop of mouthwash, seawater and vinegar

Fig.S25: Color change of Receptor R upon dry grinding of receptor with 1 eq. of TBAAcO ; R alone (left), R+ TBAAcO (right)

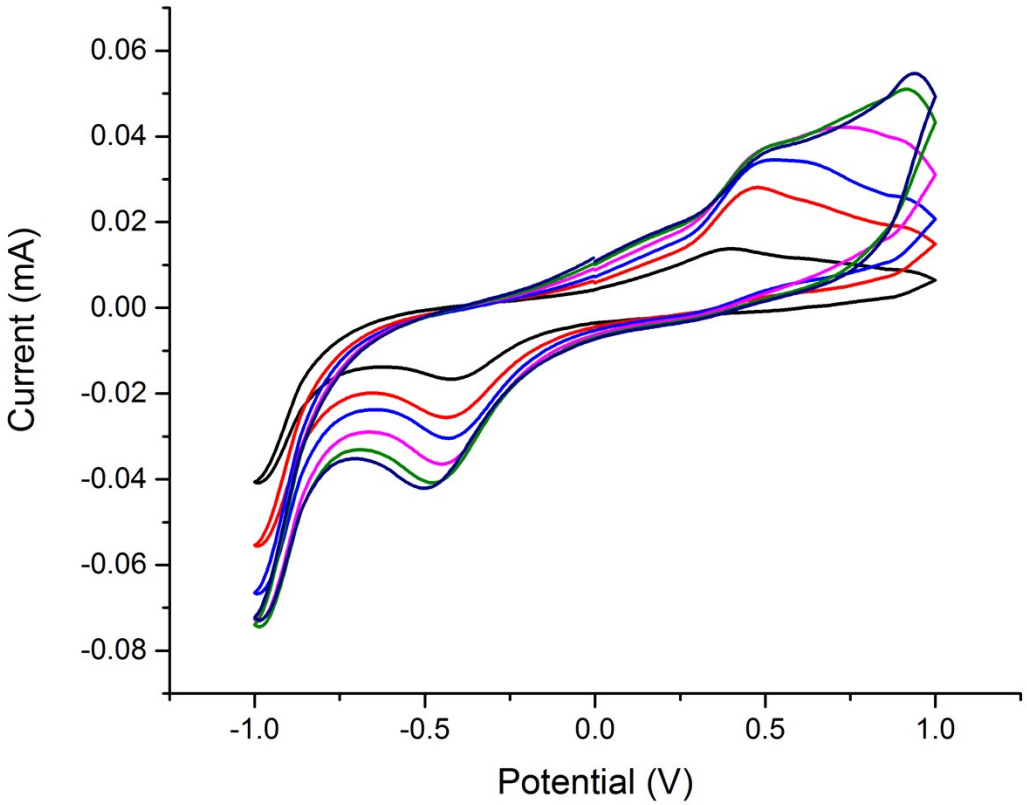

Fig.S26: Cyclic voltammogram of Receptor R (5x10 $^{-5}$M) with incremental addition of TBAAcO ion (0-1 equiv.)

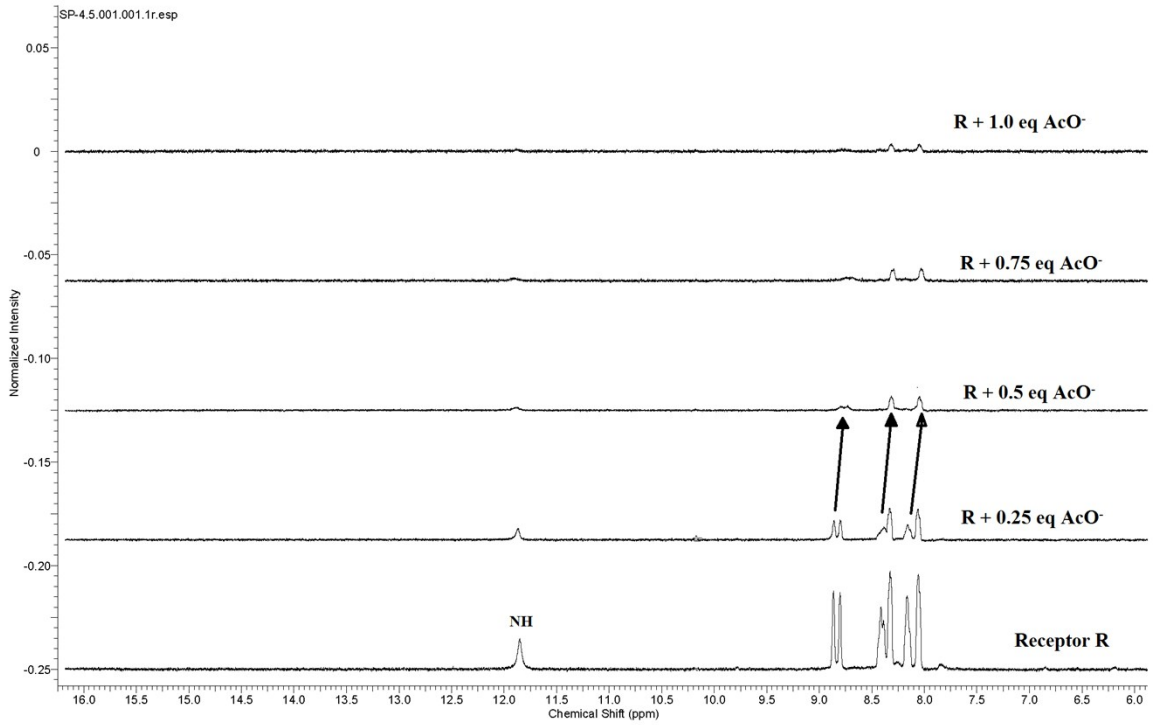

Fig. S27: ^{1}H NMR titration of receptor R with incremental addition of TBAAcO ion (0-1 eq.)

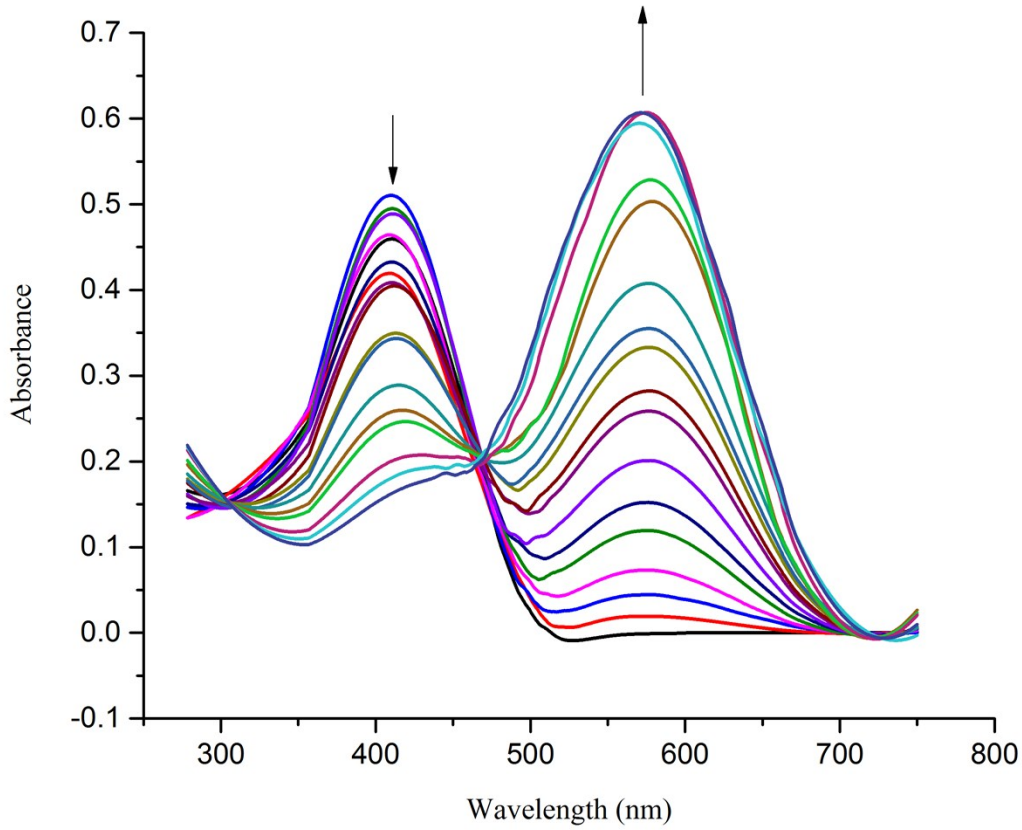

Fig. S28: UV-Vis titration spectra of R(1×10^{-4} M, DMSO) with the incremental addition of standard solution of TBAOH (1×10^{-2}M in DMSO)

Calculation of binding constant:

Binding constant has been calculated using B-H equation[4] (Eq.1).

$1/(A-A_o) = 1/(A_{max} - A_o) + 1/K [F^-]^n (A_{max} - A_o)$ ---------- (Eq.1)

Where, A_0, A, A_{max} are the absorption considered in the absence of F^-, at an intermediate, and at a concentration of saturation. K is binding constant, $[F^-]$ is concentration of F^- ion and n is the stoichiometric ratio.

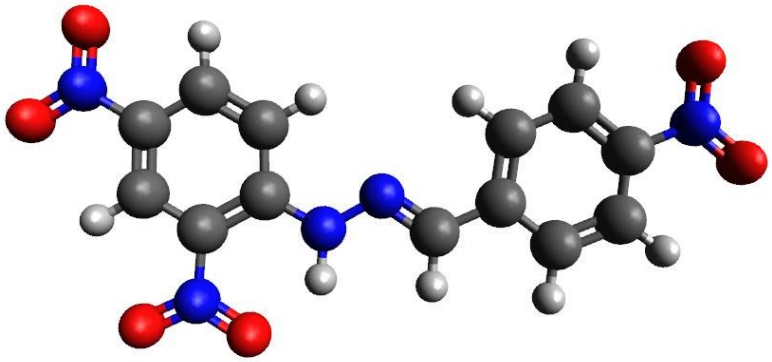

Fig. S29: Optimized geometry of the receptor in gas phase

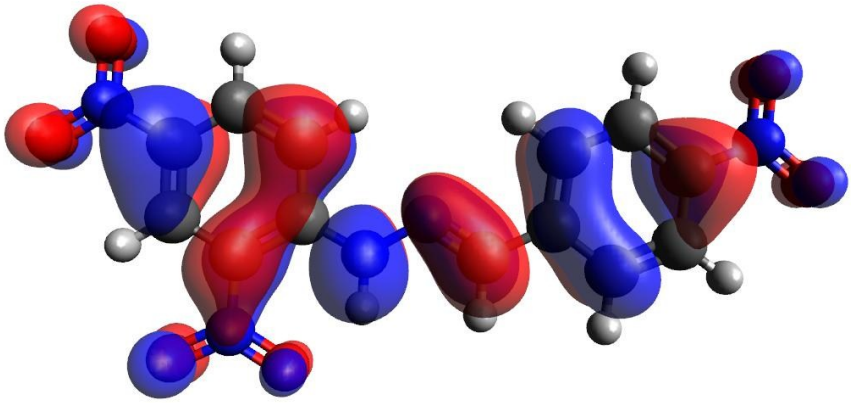

Fig. S30: HOMO of the receptor in gas phase

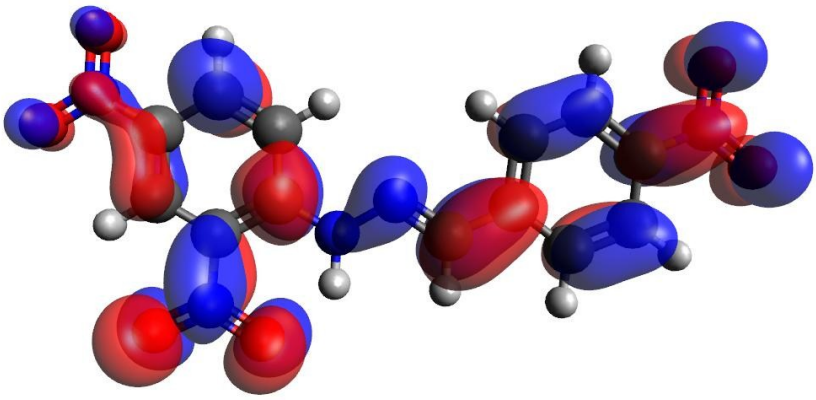

Fig. S31: LUMO of the receptor in gas phase

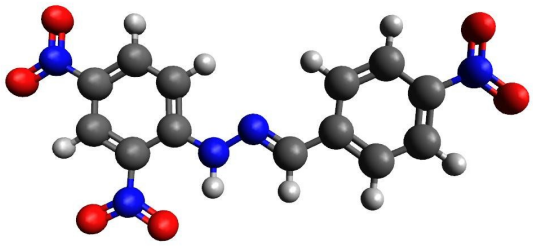

Fig. S32: Optimized structure of the receptor in DMSO

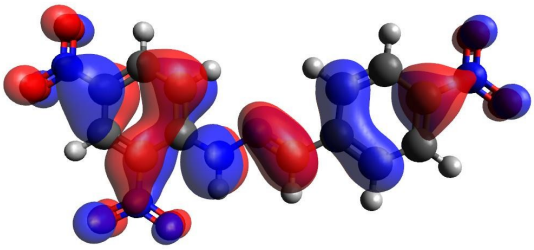

Fig. S33: HOMO of the receptor in DMSO

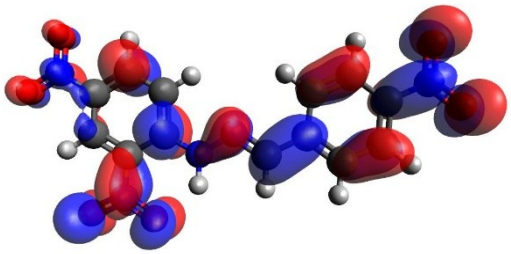

Fig. S34: LUMO of the receptor in DMSO

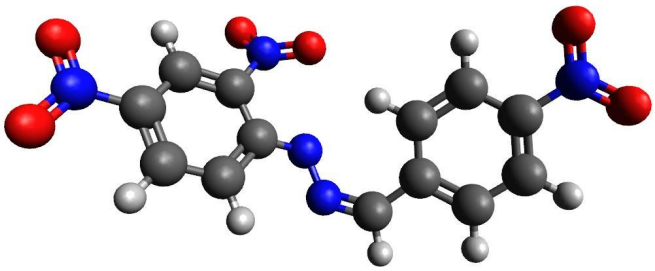

Fig. S35: Optimized structure of the deprotonated receptor in acetone

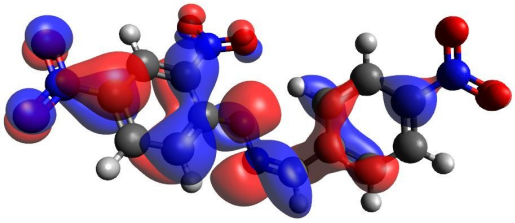

Fig. S36: HOMO of the deprotonated receptor in acetone

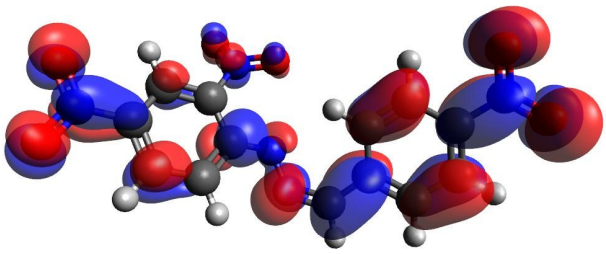

Fig. S37: LUMO of the deprotonated receptor in acetone

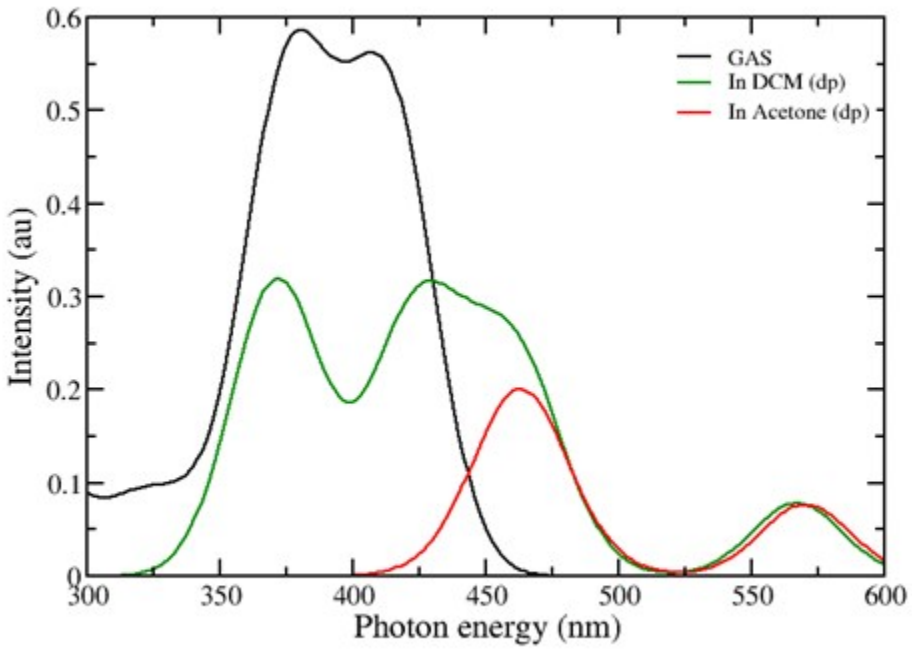

Fig. S38: UV-Vis spectra of the receptor in gas phase, in solvents such as DCM and acetone with addition of AcO^- ion

Table S1: Changes in absorption maxima of receptor R in various solvents upon addition of 1eq. of TBAAcO in dry DMSO

Solvent	Dielectric constant	λ_{max} (nm)
1,4-dioxane	2.21	553
Tetrahydrofuran	7.58	587
Dichloromethane	8.93	564
Acetone	20.70	569
Acetonitrile	37.50	563
Dimethylsulfoxide	46.80	576

Table S2: Binding ratio, binding constant and detection limit of receptor R

Anion	Media	Binding ratio	Binding constant	Detection limit (ppm)
AcO (TBA^+)	DMSO	1:1	$5.28 \times 10^4\ M^{-1}$	1.5
AcO (Na^+)	DMSO:H_2O (9:1 v/v)	1:1	$3 \times 10^4\ M^{-1}$	0.8
AcO (TBA^+)	DMSO:Tris HCl (9:1 v/v)	1:1	$1.33 \times 10^2\ M^{-1}$	15
F (TBA^+)	DMSO	1:1	$1.1 \times 10^2\ M^{-1}$	2.5
F (Na^+)	DMSO:H_2O (9:1 v/v)	1:1	$4.2 \times 10^4\ M^{-1}$	0.4
H_2PO_4 (TBA^+)	DMSO	1:1	$3.15 \times 10^2\ M^{-1}$	3.3

Table S3: Mullliken charge distribution and spin densities derived from DFT calculations

S.No.	Atom	Atomic charges		Atomic charges		Spin densities	
		Gas phase	DMSO	DCM	Acetone	DCM	Acetone
1	C	0.158453	0.16084	0.920518	0.941286	0.012169	0.014439
2	C	-0.047047	-1.08816	-0.63433	-0.64206	0.016148	0.014544
3	C	0.038748	0.77922	0.305825	0.315782	-0.00678	-0.00585
4	C	0.278998	-0.90151	-0.26357	-0.27774	0.015779	0.014088
5	C	0.04204	0.117055	0.029906	0.025072	-0.01167	-0.01084
6	C	-0.008876	0.641967	0.758474	0.763879	0.016737	0.015312
7	C	0.179414	-0.34923	-0.60375	-0.60437	0.044722	0.039426
8	C	0.403362	0.023445	-0.2458	-0.24275	-0.20273	-0.19967
9	C	0.008033	0.812116	1.175843	1.219832	0.239271	0.239158
10	C	0.054795	-0.1579	0.203773	0.209165	-0.07132	-0.07008
11	C	0.280735	-0.33983	-0.20175	-0.21337	0.15687	0.155579
12	C	0.025901	0.424902	0.39737	0.399078	-0.08735	-0.08813
13	C	0.248575	-0.04609	-0.76707	-0.79856	0.137724	0.135384
14	N	0.381867	-0.26395	-0.24661	-0.24065	-0.00059	-0.00045

15	N	-0.190539	-0.15194	0.272571	0.275278	0.19691	0.203543
16	N	0.380256	-0.4565	-0.25026	-0.25037	0.485658	0.482539
17	N	0.377313	-0.28258	-0.26105	-0.25462	-0.00719	-0.00661
18	N	-0.222821	0.441835	-0.31744	-0.31412	-0.0093	-0.00892
19	O	-0.391404	-0.07048	-0.06206	-0.06759	0.002256	0.002106
20	O	-0.390718	-0.06823	-0.06452	-0.07098	0.002202	0.002035
21	O	-0.395056	-0.08055	-0.06392	-0.06953	0.021514	0.022096
22	O	-0.392518	-0.07896	-0.05798	-0.06503	0.025248	0.025941
23	O	-0.375782	-0.00719	0.015077	0.007395	0.019981	0.020152
24	O	-0.443727	-0.05828	-0.03926	-0.04504	0.003744	0.004206

References:

[1] A.D. Becke, Density-functional thermochemistry .III. The role of exact exchange, J. Chem. Phys. 98 (1993) 5648–5652.

[2] C. Lee, W. Yang, R.G. Parr, Development of the Colle-Salvetti correlation-energy formula into a functional of the electron density**,** Phys. Rev. B 37 (1988) 785–789.

[3] J.P. Perdew, Y. Wang, Accurate and simple analytic representation of the electron-gas correlation energy Phys. Rev. B 45 (1992) 13244–13249

[4] H. Benesi and H. Hildebrand, J. Am. Chem. Soc., 1948, 71, 2703–2707.